Redox Biology 75 (2024) 103287

Contents lists available at ScienceDirect

Redox Biology

journal homepage: www.elsevier.com/locate/redox

The deubiquitinase OTUD1 stabilizes NRF2 to alleviate hepatic ischemia/reperfusion injury

Qi Zhang [a,b,c,1], Zihan Chen [a,1], Jinglei Li [b], Kunpeng Huang [b], Zhihao Ding [d], Biao Chen [b], Tianxing Ren [b], Peng Xu [b], Guoliang Wang [e], Hongji Zhang [f], Xiao-Dong Zhang [g], Jinxiang Zhang [b,**], Hui Wang [a,b,*]

[a] Department of Medical Genetics, School of Basic Medicine, Tongji Medical College, Huazhong University of Science and Technology, Wuhan, 430030, China
[b] Department of Emergency Surgery, Union Hospital, Tongji Medical College, Huazhong University of Science and Technology, Wuhan, 430022, China
[c] National "111" Center for Cellular Regulation and Molecular Pharmaceutics, Key Laboratory of Fermentation Engineering (Ministry of Education), Hubei University of Technology, Wuhan, 430068, China
[d] Hubei Key Laboratory of Cell Homeostasis, College of Life Sciences, Wuhan University, Wuhan, 430072, China
[e] Department of Hepatobiliary Surgery, Union Hospital, Tongji Medical College, Huazhong University of Science and Technology, Wuhan, 430022, China
[f] Department of Surgery, University of Virginia, Charlottesville, VA, 22903, USA
[g] Hengyang Medical School, University of South China, Hengyang, 421001, China

ARTICLE INFO

Keywords:
OTU deubiquitinase 1
Deubiquitination
Hypoxia/oxygenation
Oxidative stress
ETGE peptides

ABSTRACT

Hepatic ischemia/reperfusion (I/R) injury is an important cause of liver function impairment following liver surgery. The ubiquitin-proteasome system (UPS) plays a crucial role in protein quality control and has substantial impact on the hepatic I/R process. Although OTU deubiquitinase 1 (OTUD1) is involved in diverse biological processes, its specific functional implications in hepatic I/R are not yet fully understood. This study demonstrates that OTUD1 alleviates oxidative stress, apoptosis, and inflammation induced by hepatic I/R injury. Mechanistically, OTUD1 deubiquitinates and activates nuclear factor erythroid 2-related factor 2 (NRF2) through its catalytic site cysteine 320 residue and ETGE motif, thereby attenuating hepatic I/R injury. Additionally, administration of a short peptide containing the ETGE motif significantly mitigates hepatic I/R injury in mice. Overall, our study elucidates the mechanism and role of OTUD1 in ameliorating hepatic I/R injury, providing a theoretical basis for potential treatment using ETGE-peptide.

1. Introduction

Hepatic ischemia/reperfusion (I/R) injury is an intrinsic phenomenon observed during liver surgeries such as liver tumor resection and transplantation [1], serving as the primary underlying cause for early allograft dysfunction or rejection in the liver [2,3]. Initially, hypoxia resulting from interrupted blood flow hampers oxygen supply, and subsequent restoration of blood supply induces profound oxidative stress and triggers inflammatory responses that activate immune cells leading to cytokine/chemokine release and apoptosis [4,5]. Hence, alleviating hepatic I/R injury can be achieved through strategies targeting reduction of oxidative stress, inflammation and apoptosis.

The ubiquitin-proteasome system (UPS) serves as an integrated protein quality control network in nearly all aspects of eukaryotic life, including I/R injury [6,7]. Deubiquitinases (DUBs) are essential components of UPS and regulate various cellular processes, including protein homeostasis, signal transduction, cell proliferation by removing ubiquitin from substrates [8]. Aberrant DUB activity is associated with numerous pathologies. Thus, DUBs have become important targets for drug development. Recent researches have revealed distinct roles for DUBs such as OTUD4 and USP29 played in the hepatic I/R process [9,10]. Therefore, understanding the role of DUBs in hepatic I/R injury is crucial for advancing clinical treatments.

In this study, we noticed that OTU deubiquitinase 1 (OTUD1) displayed the most significant transcriptional differences among DUBs during hepatic I/R procedure. Meanwhile, previous studies have

* Corresponding author. 13 Hangkong Road, Wuhan, Hubei Province, 430022, China.
** Corresponding author. 1277 Jiefang Road, Wuhan, Hubei Province, 430022, China.
E-mail addresses: zhangjinxiang@hust.edu.cn (J. Zhang), wanghuipitt@hust.edu.cn (H. Wang).
[1] These authors contributed equally: Qi Zhang, Zihan Chen.

https://doi.org/10.1016/j.redox.2024.103287
Received 3 July 2024; Accepted 26 July 2024
Available online 26 July 2024

demonstrated that *Otud1* knockout mice were more susceptible to lipopolysaccharide (LPS)-induced sepsis [11], and loss-of-function mutations of OTUD1 enhanced immune response and were associated with autoimmunity [12], suggesting a potential role for OTUD1 in hepatic inflammation caused by I/R. Additionally, our findings indicate that besides its upregulation, OTUD1 also contributes to improved liver function in patients undergoing hepatectomy. Therefore, further investigation is necessary to elucidate the specific function and underlying mechanism of OTUD1 in hepatic I/R insults.

Nuclear factor E2-related factor 2 (NRF2) is a pivotal transcription factor involved in counteracting oxidant stress [13]. Treatment with NRF2 agonists itaconate or sulforaphane has been demonstrated to alleviate hepatic I/R injury in mice [14,15], while deficiency of NRF2 in donor liver exacerbates I/R injury in recipients among transplant recipients [16], suggesting that enhancing NRF2 activity may attenuate hepatic I/R injury. The regulation of NRF2 activity occurs at multiple levels encompassing proteasomal protein degradation, transcriptional control, and post-transcriptional modifications [17,18]. Notably, NRF2 activation are tightly governed by its primary negative modulator, the E3 ligase adaptor Kelch-like ECH-associated protein 1 (KEAP1), which plays a pivotal role not only in maintaining intracellular redox balance but also regulating inflammatory responses [19]. Under homeostatic conditions, NRF2 undergoes ubiquitination by KEAP1/cullin 3 (CUL3) E3 ligase and followed by subsequent targeting for proteasomal degradation [20]. However, mild oxidative stress and certain deubiquitinase such as DUB3 and USP11 have been documented to facilitate the escape of NRF2 proteins from KEAP1/CUL3-mediated ubiquitination, resulting in initiation of downstream gene cascades harboring antioxidant response elements (AREs) [21–23]. These collective findings promoted us to investigate the regulatory mechanism by which deubiquitinase

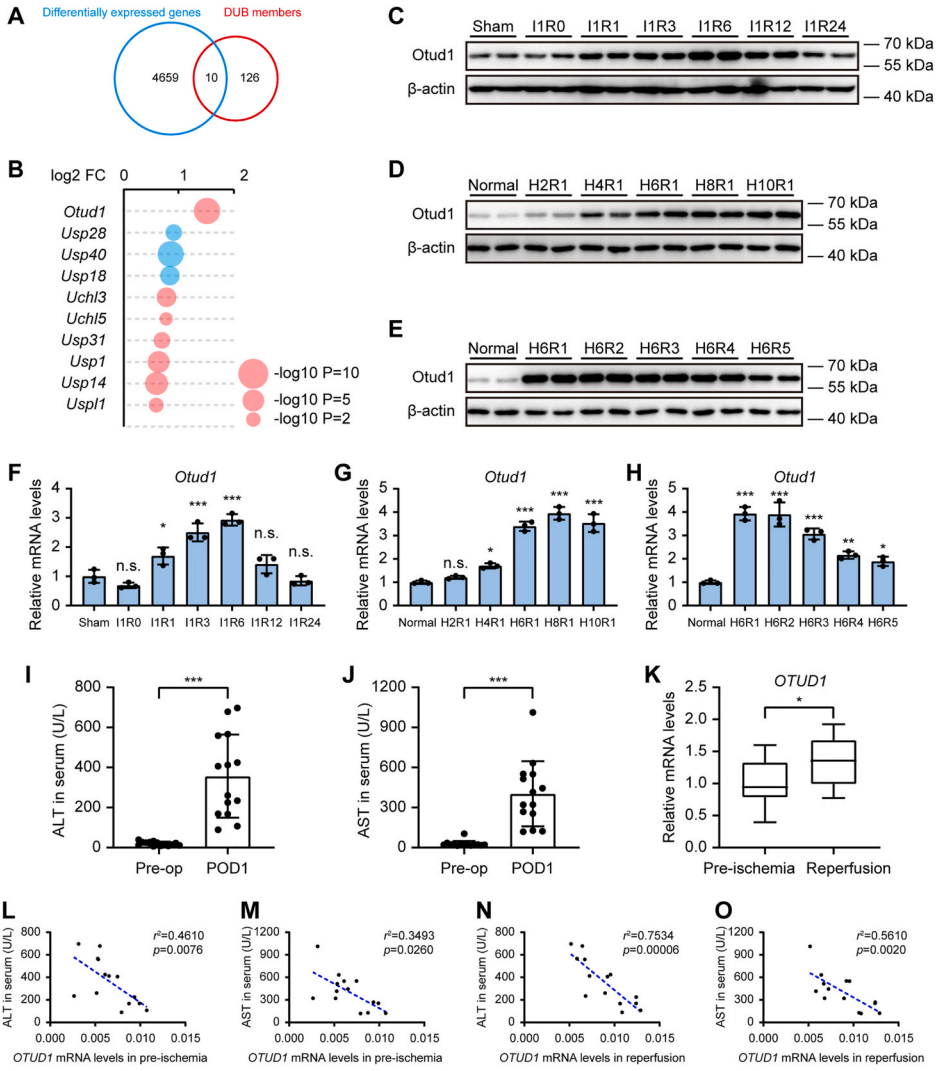

Fig. 1. OTUD1 is upregulated during hepatic I/R injury. A) Venn diagram showing the number of differentially expressed genes (cutoff fold change >1.5 and $p < 0.05$) in response to hepatic I/R (I1R6) injury (blue), DUB members (red) and overlapping genes in the datasets. B) Bubble chart of ten of the differentially expressed DUB genes in response to murine hepatic I/R (I1R6) injury (red, upregulated; blue, downregulated). C-H) WT mice were subjected to sham treatment or ischemia for 1 h followed by reperfusion for 0, 1, 3, 6, 12 or 24 h (I1R0, ischemia for 1 h followed by reperfusion for 0 h). Primary hepatocytes were subjected to normal treatment or H/R treatments for the indicated times (H2R1, hypoxia for 2 h followed by reperfusion for 1 h). Otud1 protein levels (C–E) and mRNA levels (F-H) in I/R or H/R models (n = 3/group). I-J) Serum ALT and AST levels of 14 hepatectomy patients (n = 14; pre-op, pre-operation; POD1, the first day postoperatively). K) *OTUD1* mRNA levels in liver samples obtained from hepatectomy patients before hepatic portal vein occlusion (pre-ischemia) and after the first time of reperfusion (reperfusion) (n = 14). L-M) The ratio of *OTUD1* mRNA levels in pre-ischemia stage negatively correlated with ALT and AST in serum at POD1 (n = 14). N-O) The ratio of *OTUD1* mRNA levels in reperfusion stage negatively correlated with ALT and AST in serum at POD1 (n = 14). For (F-H), the significance was determined by one-way ANOVA; for (I-K), the significance was determined by Student's two-tailed *t*-test; for (L–O), Spearman correlation analysis was employed. $*p < 0.05$, $**p < 0.01$, $***p < 0.001$, n.s. non-significant. (For interpretation of the references to colour in this figure legend, the reader is referred to the Web version of this article.)

OTUD1 activates NRF2 in the pathogenesis of hepatic I/R injury.

Here, we have demonstrated that OTUD1 functions as a specific DUB for NRF2, leading to the stabilization and activation of the NRF2/ARE pathway, thereby results in the reduction of oxidative stress, apoptosis and inflammation in I/R-challenged liver. Notably, ETGE peptides derived from OTUD1 show promise in attenuating hepatic I/R injury and may hold potential as an effective therapeutic intervention for this condition.

2. Results

2.1. OTUD1 is upregulated during hepatic I/R injury

It has been reported that proteasome inhibitors could reduce hepatic I/R injury [7], similarly, DUBs facilitate the evasion of numerous proteins from proteasome-mediated degradation and may exert protective effects in hepatic I/R injury. To identify essential DUBs involved in hepatic I/R injury, we conducted transcriptomic analyses of liver samples from mice subjected to hepatic I/R-challenged (ischemia for 1 h followed by reperfusion for 6 h) and sham-operated mice. The RNA-seq data has been deposited in the National Center for Biotechnology Information (NCBI) Sequence Read Archive (SRA) database (PRJNA973131). Differentially expressed genes (DEGs) were screened by comparing the I/R group versus the sham group using a cutoff fold change >1.5 and $p < 0.05$. Common genes were further screened from the aforementioned DEGs and DUB members (Fig. 1A). Of those differentially expressed DUB genes, *Otud1* was the most significantly increased member (Fig. 1B). In order to explore in which type of cells the upregulation of *Otud1* occurred, we isolated primary hepatocytes and non-parenchymal cells (NPCs) from hepatic I/R-challenged mice and sham-operated mice to detect the mRNA and protein levels of Otud1. The results showed that Otud1 was upregulated in hepatocytes rather than NPCs (Figs. S1A–D), thus, we focused on hepatocytes to explore the function of OTUD1 in hepatic I/R process. Consistent with the transcriptomic data, Otud1 mRNA and protein levels were both increased during hepatic I/R and primary hepatocytes hypoxia/oxygenation (H/R) procedures (Fig. 1C–H). Additionally, Otud1 expression peaked at 6 h of reperfusion after 1 h ischemia, which coincided with the most severe hepatic injury timepoint in murine hepatic I/R model [24], suggesting the involvement of OTUD1 in hepatic I/R injury. Subsequently, we analyzed the correlation between OTUD1 levels and liver function using samples from patients who underwent partial hepatic resection at Wuhan Union Hospital (Table S1). The serum levels of alanine aminotransferase (ALT) and aspartate transaminase (AST) peaked on the first postoperative day (POD1), following gradually decreasing to preoperative levels over the subsequent days (Fig. 1I–J and S2A-B). Notably, *OTUD1* mRNA levels were obviously upregulated in the liver after reperfusion compared to pre-ischemia conditions (Fig. 1K). Moreover, higher expression of *OTUD1* in the liver, whether before ischemia or during reperfusion stage, was associated with lower serum ALT and AST levels on POD1 respectively (Fig. 1L–O). These findings suggest that OTUD1 is up-regulated in the setting of hepatic I/R injury and contributes to favorable liver function.

2.2. OTUD1 protects against hepatic I/R injury

To investigate the specific role of OTUD1 in hepatic I/R injury, global *Otud1*-knockout (*Otud1*-KO) mice were generated using CRISPR-Cas9 genome editing system (Fig. S3A). Genotyping result revealed an 8509-base deletion at *Otud1* gene in *Otud1*-KO mice (Fig. S3B), and qPCR assay further confirmed successful knockout of *Otud1* (Fig. S3C). The earliest research about OTUD1 KO mice that endogenous OTUD1 deficiency promoted SeV-induced IFNβ production [25]. In this study, we utilized WT and *Otud1*-KO mice to establish a hepatic I/R model, and our findings indicated that compared to WT mice, Otud1 deficiency exacerbated hepatic I/R injury as evidenced by elevated serum ALT and AST levels, as well as larger necrotic areas (Fig. 2A and B). Hepatocyte apoptosis is a hallmark of hepatic I/R injury [4]. TUNEL staining was conducted to assess hepatocyte apoptosis. Our findings demonstrated that Otud1 deficient mice exhibited an augmented number of TUNEL-positive apoptotic cells (Fig. 2C), heightened levels of pro-apoptotic proteins (Bax, cleaved caspase3 and cleaved PARP), and reduced levels of the anti-apoptotic protein Bcl2 in comparison to WT mice undergoing hepatic I/R operation (Fig. 2D). Similarly, primary hepatocytes lacking Otud1 displayed increased expression of pro-apoptotic proteins but decreased level of the anti-apoptotic protein Bcl2 when compared to WT hepatocytes under H/R stimulation (Fig. 2E). Additionally, serum levels of inflammatory cytokines, including IL-6, MCP-1, IFN-γ, TNF and IL-12p70, were remarkably upregulated in *Otud1*-KO mice compared with those in WT mice after being challenged with hepatic I/R (Fig. 2F). Taken together, these findings indicate that OTUD1 depletion exacerbates hepatic I/R injury, apoptosis and inflammation.

Subsequently, we investigate whether overexpression of OTUD1 can mitigate hepatic I/R injury. Otud1-overexpressing mice and control mice were generated by injecting recombinant adenovirus Ad-Otud1 or Ad-GFP into WT mice, followed by hepatic I/R operation. The results showed that Otud1 overexpression led to a reduction in serum ALT and AST levels (Fig. 3A), as well as a decrease in liver tissue necrosis and apoptosis induced by hepatic I/R compared to control mice (Fig. 3B and C). Consistently, Otud1 overexpression resulted in decreased levels of pro-apoptotic proteins and increased expression of anti-apoptotic protein Bcl2 in I/R-challenged liver samples or H/R-treated primary hepatocytes (Fig. 3D and E). Moreover, Otud1 overexpression markedly downregulated cytokines induced by hepatic I/R treatment (Fig. 3F).

As mentioned previously, oxidative stress is considered a pivotal indicator of hepatic I/R injury [4]. We also utilized the dihydroethidium (DHE) probe to measure the levels of ROS in liver samples subjected to I/R. The results revealed that *Otud1*-KO mice exhibited higher ROS levels compared to WT mice following I/R treatment (Fig. S4A). Consistently, Otud1 overexpression led to a decrease of ROS in I/R-challenged liver samples (Fig. S4B). Taken together, these findings demonstrate that OTUD1 provides protection against oxidative stress induced by hepatic I/R.

2.3. OTUD1 protects hepatocytes against oxidative stress and apoptosis induced by H/R

To assess the capacity of OTUD1 in mitigating hepatocyte damage under H/R conditions, we generated Otud1-knockdown or Otud1 overexpression AML12 cells (murine hepatocytes cell line) by infecting with pLKO.1-sh-Otud1 or pHAGE-Otud1 respectively. The cells were subjected to 6 h hypoxia followed by 1 h of reoxygenation to simulate an *in vitro* hepatic I/R model [26]. The efficiency of Otud1 knockdown and overexpression was confirmed through quantification of Otud1 protein levels (Figs. S5A and D). Our results showed that compared to control cells, Otud1 knockdown led to an increase in apoptotic cells (Figs. S5B–C), while Otud1 overexpression resulted in a decrease in apoptotic cells induced by H/R exposure (Figs. S5E–F). Keeping in line with these results, Otud1 overexpression suppressed the upregulation of pro-apoptotic proteins and prevented the reduction of anti-apoptotic protein Bcl2 caused by H/R treatment (Fig. S5G). Collectively, these findings strongly support the role of OTUD1 as an inhibitor of hepatocyte apoptosis under H/R conditions.

Given the fact that oxidative stress typically results in mitochondrial damage in cells [27]. We sought to investigate whether OTUD1 confers defense against mitochondria damage caused by oxidative stress. Mitochondrial membrane potential (MMP) and ROS levels serve as sensitive indicators of mitochondrial damage, thus JC-1 and H2DCFDA probes were employed to quantify MMP and ROS levels under hepatocyte H/R stimulation respectively. As expected, Otud1 knockdown further reduced MMP (Figs. S6A–B) and elevated ROS levels (Fig. S6C)

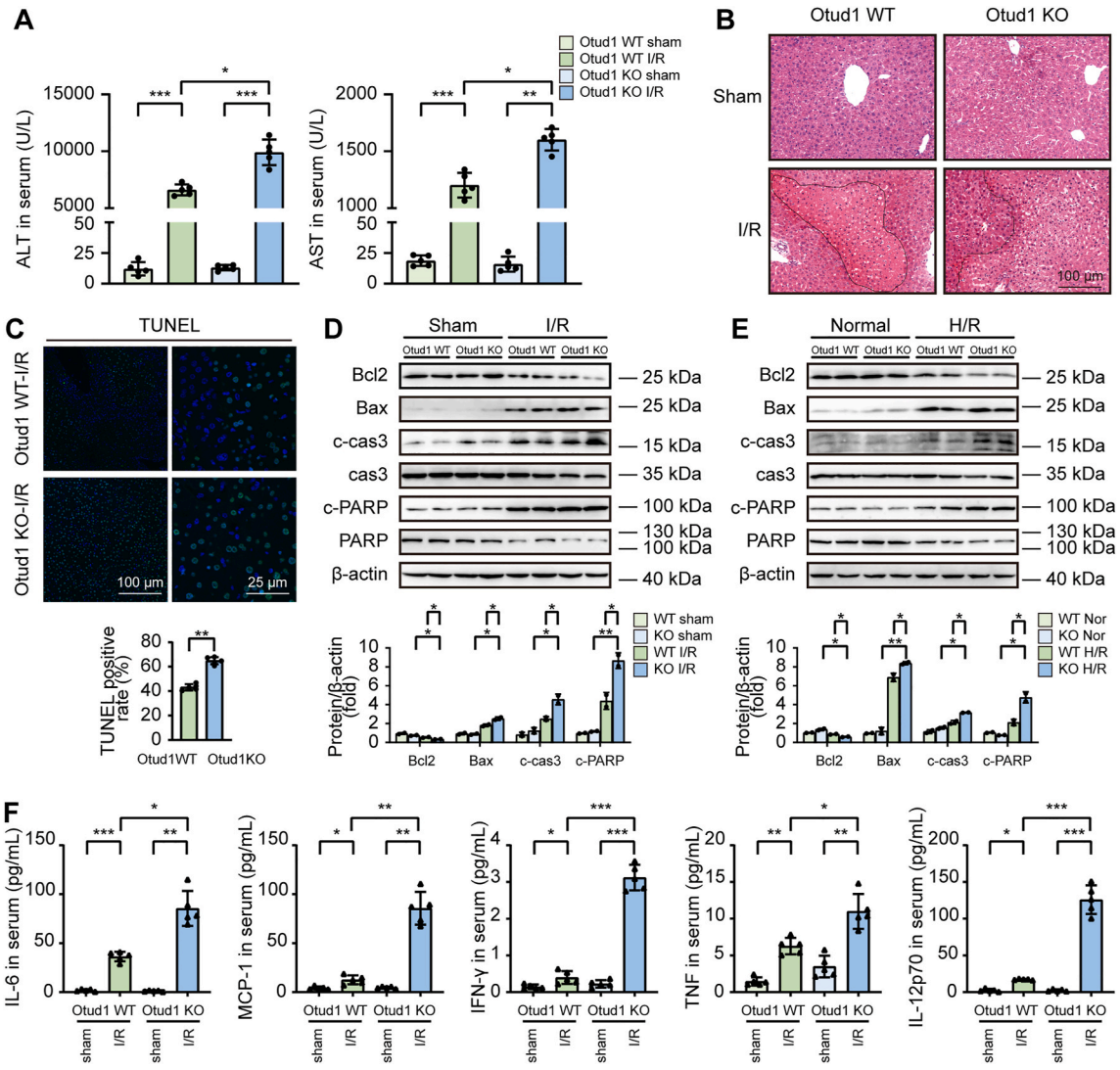

Fig. 2. OTUD1 deficiency aggravates hepatic I/R injury. A) Serum ALT and AST levels of Otud1 WT and Otud1 KO mice subjected to sham or hepatic I/R (I1R6) operation (n = 5/group). B) Representative histological H&E staining images of liver sections from Otud1 WT and Otud1 KO mice subjected to sham or hepatic I/R operation (n = 5/group). C) Representative TUNEL staining images of liver sections from Otud1 WT and Otud1 KO mice subjected to hepatic I/R operation (n = 5/group). D-E) Pro-apoptosis and anti-apoptosis protein levels in liver samples (D) and primary hepatocytes (E) from Otud1 WT and Otud1 KO mice subjected to hepatic I/R operation or hepatocyte H/R (H6R1) treatment (n = 5/group). F) Serum inflammatory factor levels in Otud1 WT and Otud1 KO mice subjected to sham or hepatic I/R operation (n = 5/group). For (A, D, E, F), the significance was determined by one-way ANOVA; for (C), the significance was determined by Student's two-tailed *t*-test. $^{*}p < 0.05$, $^{**}p < 0.01$, $^{***}p < 0.001$, n.s. non-significant.

in AML12 cells induced by H/R treatment in comparison with control cells. Conversely, Otud1 overexpression exhibited the opposite effect (Figs. S6D–F). These findings indicate that OTUD1 attenuates mitochondria damage caused by oxidative stress following H/R treatment *in vitro*.

2.4. OTUD1 mitigates hepatocyte H/R injury by activating NRF2/ARE pathway

Next, we investigated the specific signaling pathway activated by OTUD1 in hepatocytes under H/R exposure. OTUD1-activated signaling pathways were screened in HEK293T cells using luciferase reporter assay employing a vector library containing 44 individual transcription factor binding elements. Among the nine signaling pathways activated by OTUD1, NRF2, a well-known antagonist of oxidant stress, exhibited a six-fold increase in transcription activity (Fig. 4A and Table S2). As a result, our study focused on the regulation of OTUD1 on NRF2 and its downstream signaling cascade. As expected, OTUD1 dose-dependently increased the protein level of NRF2 (Fig. 4B). Given that OTUD1 possess DUB activity, we investigated whether it upregulates NRF2 level by stabilizing NRF2. We utilized cycloheximide (CHX) to inhibit protein translation and observed that OTUD1 overexpression dramatically prolonged the half-life of NRF2 protein in AML12 cells (Fig. 4C), signifying its role in stabilizing NRF2. As a transcription factor, NRF2 is known to counteract oxidant stress by translocating to nucleus and facilitating the expression of downstream genes with ARE, such as *HO-1*, *NQO1* etc [21]. We therefore explored whether OTUD1 promoted nuclear translocation of NRF2 and enhanced the expression of downstream genes with ARE in AML12 cells. Nucleocytoplasmic separation experiments showed that OTUD1 enhanced NRF2 nuclear accumulation (Fig. 4D). In addition, OTUD1 upregulated protein and mRNA levels of downstream targets (HO-1 and NQO1) of NRF2 in AML12 cells in a dose-dependent manner (Fig. 4B, 4E-F). Likewise, in human samples, there was a positive correlation between expressions of OTUD1 and NRF2 in liver sections from patients who underwent hepatic I/R injury for hepatectomy (Fig. 4G and H). These findings indicate that OTUD1

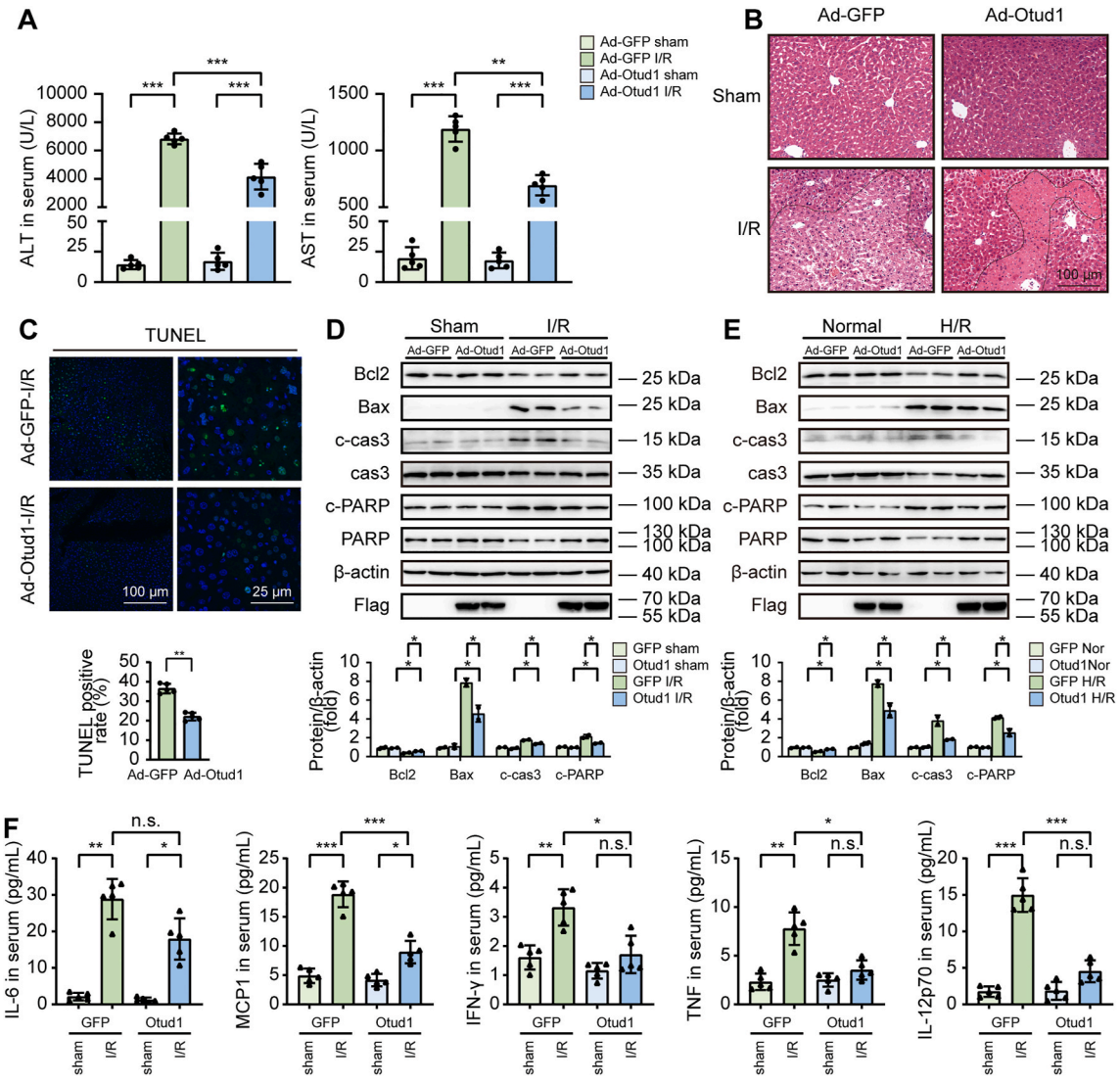

Fig. 3. OTUD1 protects against hepatic I/R injury. A) WT mice were infected with control adenovirus (Ad-GFP) or adenovirus expressing Otud1 (Ad-Otud1). Serum ALT and AST levels of Ad-GFP and Ad-Otud1 mice subjected to sham or hepatic I/R (I1/R6) operation (n = 5/group). B) Representative histological H&E staining images of liver sections from Ad-GFP and Ad-Otud1 mice subjected to sham or hepatic I/R operation (n = 5/group). C) Representative TUNEL staining images of liver sections from Ad-GFP and Ad-Otud1 mice subjected to sham or hepatic I/R operation (n = 5/group). D-E) Pro-apoptosis and anti-apoptosis protein levels in liver samples (D) and primary hepatocytes (E) from Ad-GFP and Ad-Otud1 mice subjected to hepatic I/R operation or hepatocyte H/R (H6R1) treatment (n = 5/group). F) Serum inflammatory factor levels in Ad-GFP and Ad-Otud1 mice subjected to sham or hepatic I/R operation (n = 5/group). For (A, D, E, F), the significance was determined by one-way ANOVA; for (C), the significance was determined by Student's two-tailed *t*-test. $^{*}p < 0.05$, $^{**}p < 0.01$, $^{***}p < 0.001$, n.s. non-significant.

stabilizes and activates NRF2/ARE pathway in hepatocytes.

We subsequently investigated whether the protective effect of OTUD1 against hepatocyte H/R injury depended on NRF2 activation. Primary hepatocytes were isolated from Nrf2-WT and Nrf2-KO mice, which were injected with Ad-GFP or Ad-Otud1 via tail vein and subjected to H/R treatment. Our findings revealed that Nrf2 depletion abrogated the suppressive effect of Otud1 on apoptosis in H/R-treated primary hepatocytes (Fig. 4I and J). In addition, Nrf2 deletion impaired Otud1 ability in reducing pro-apoptotic proteins and elevating anti-apoptotic protein Bcl2 in H/R-stimulated primary hepatocytes (Fig. S7A). Nrf2 silence also nullified Otud1 activity in upregulating Ho-1 and Nqo1 proteins (Fig. S7B), as well as in downregulating ROS production under H/R treatment (Fig. S7C). These observations indicate that OTUD1 protects hepatocytes from H/R injury by activating NRF2/ARE pathway.

2.5. OTUD1 stabilizes NRF2 through its C320 catalytic residue and ETGE motif

OTUD1 has been validated to stabilize and activate NRF2, functioning as a protective regulator in liver I/R process (Fig. 4). Considering that OTUD1 possess DUB activity [28] and NRF2 activation is tightly regulated by deubiquitination [22], it is postulated that OTUD1 may activate NRF2 by removing ubiquitin chains from NRF2. To test the hypothesis, we initially investigated their physical interaction and the specific region(s) responsible for the interaction. We partitioned OTUD1 into four primary regions: Ala-rich domain (amino acid (aa) 1–155 containing ETGE motif), linker region (aa 156–300), OTU region (aa 301–438 containing C320 catalytic residue) and UIM domain (aa 439–481) (Fig. 5A). Co-immunoprecipitation (co-IP) assays showed that OTU domain, but not other regions of OTUD1, interacted with NRF2 in HEK293T cells (Fig. 5B). In addition, we delineated the critical region(s) of NRF2 essential for its interaction with OTUD1. We generated three NRF2 truncations: NRF2-E (Neh2 domain deletion), NRF2-F (Neh6

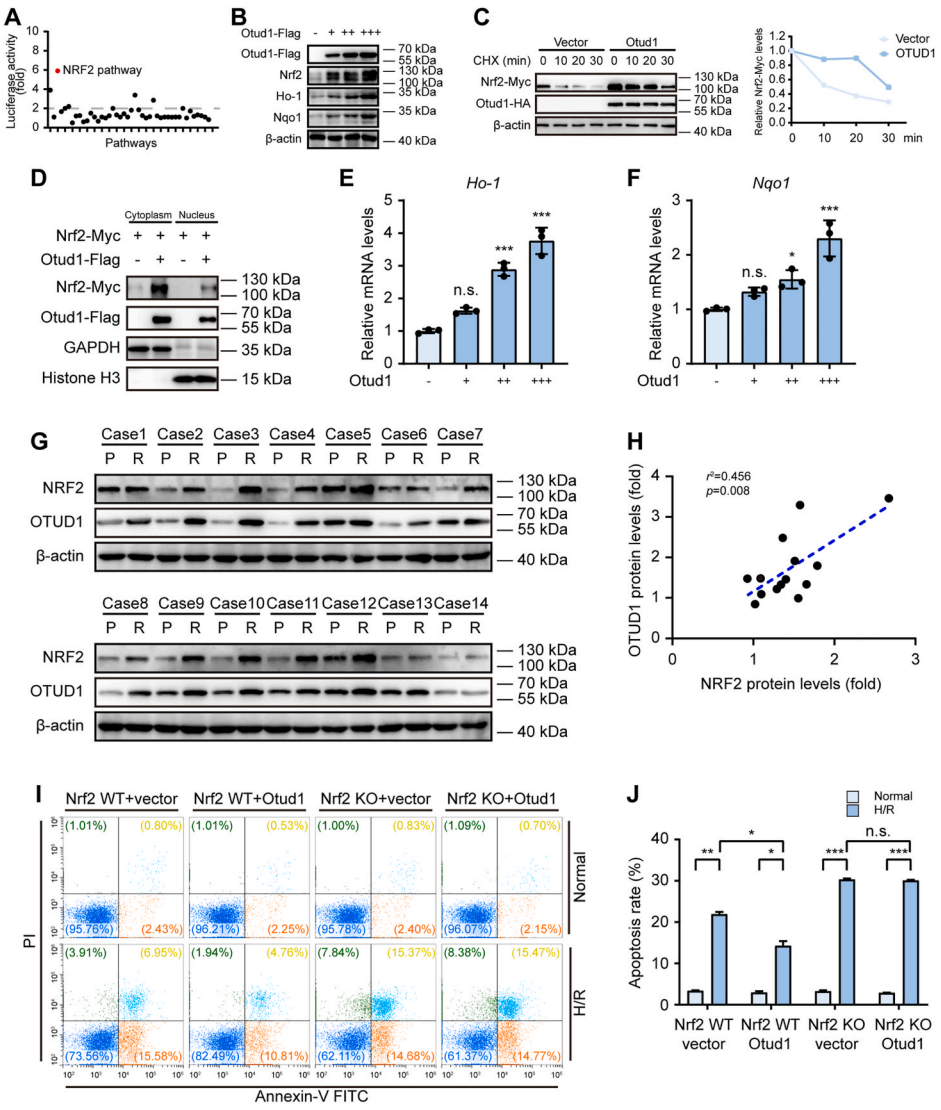

Fig. 4. OTUD1 mitigates hepatocyte H/R injury by activating NRF2/ARE pathway. A) The transcriptional activities of 44 transcription factors were measured by luciferase assay in HEK293T cells. The cutoff of 2-fold change was marked by a gray line. B) Protein levels of Otud1, Nrf2, Ho-1 and Nqo1 in Otud1-overexpressing AML12 cells. C) Nrf2-Myc degradation rate affected by Otud1 in AML12 cells. D) Nrf2-Myc protein levels in the cytoplasm and nucleus affected by Otud1 in AML12 cells. E-F) mRNA levels of *Ho-1* and *Nqo1* in Otud1-overexpressing AML12 cells. G) NRF2 and OTUD1 protein levels in liver samples obtained from hepatectomy patients (n = 14; P, pre-ischemia; R, reperfusion). H) The ratio of OTUD1 protein levels positively correlated with NRF2 protein levels in (G). I) Flow cytometry apoptosis analysis of the indicated primary hepatocytes under normal and H/R (H6R1) conditions (n = 3/group). J) Statistics showing apoptosis rate in (I). For (E, F, J), the significance was determined by one-way ANOVA; for (H), Pearson correlation analysis was employed. *$p < 0.05$, **$p < 0.01$, ***$p < 0.001$, n.s. non-significant.

domain deletion) and NRF2-G (Neh1 and 3 domains deletion) (Fig. 5C). Our findings demonstrated that the interaction between OTUD1 and NRF2 primarily occurred through its Neh2 domain (aa 1–111), as the Neh2 deletion truncation (NRF2-E) failed to bind with OTUD1 in HEK293T cells (Fig. 5D). Collectively, these results suggest a physical interaction between OTUD1 and NRF2.

Afterwards, we conducted further investigation into the critical region(s) of OTUD1 responsible for NRF2 stability. Upon analyzing the functional domains of OTUD1, we noticed that in addition to the catalytic active C320 residue in OTU domain, an ETGE motif in Ala-rich domain of OTUD1 resembled the NRF2 ETGE motif which mediated the KEAP1-NRF2 interaction [13]. Therefore, we explored whether both the C320 residue and ETGE motif of OTUD1 were necessary for NRF2 stabilization and activation. Our results showed that overexpression of OTUD1-WT strongly increased NRF2 protein levels, while overexpression of either the inactive mutant C320S (M1) or ETGE deletion mutant (M2) only slightly increased NRF2 protein levels. Furthermore, our results showed that combined mutant M3 with both inactive C320 and depleted ETGE had no ability to increase NRF2 at all (Fig. 5A,5E). Keeping in line with the data, luciferase assay revealed that overexpression of OTUD1-WT markedly enhanced NRF2 luciferase activity. The M1 and M2 mutants exhibited a much weaker effect, while the combined mutant M3 showed no ability to promote NRF2 luciferase activity (Fig. 5F). Together, these findings suggest that both the C320 residue and ETGE motif of OTUD1 are essential for NRF2 stability and activity.

Given the pivotal role of the ETGE motif in mediating NRF2 binding with KEAP1, our subsequent inquiry aimed to ascertain whether OTUD1 also interacted with KEAP1 through its ETGE motif. Co-IP results demonstrated that both OTUD1-WT and M1 mutant interacted with KEAP1, whereas the M2 and M3 mutants did not exhibit any interaction (Fig. 5G), demonstrating that the ETGE motif, rather than the C320 residue of OTUD1, which mediated its binding with KEAP1.

Given that both OTUD1 and NRF2 are linked to KEAP1 via ETGE

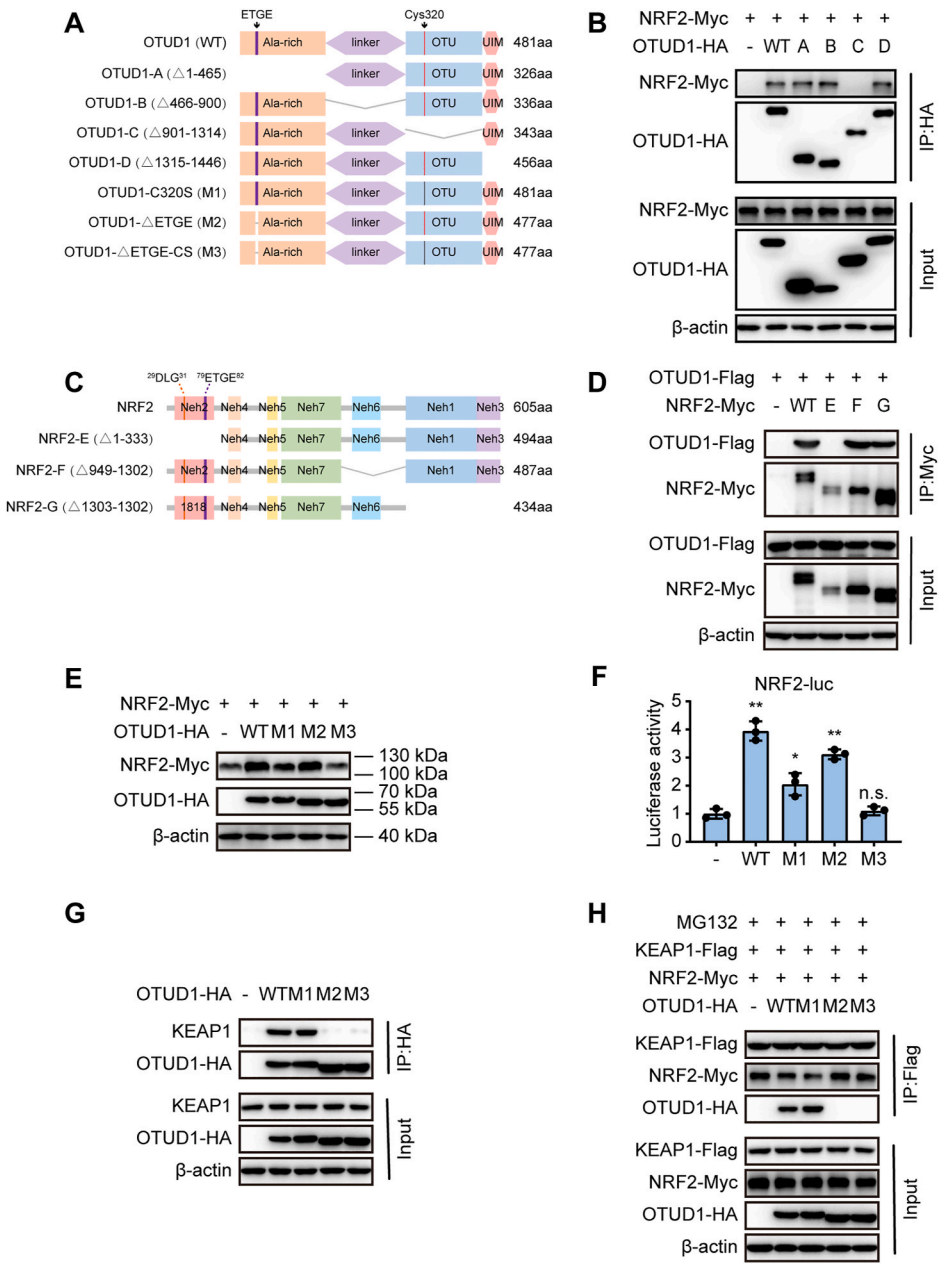

Fig. 5. OTUD1 stabilizes NRF2 through its C320 catalytic residue and ETGE motif. A) Schematic representation of full-length and truncated OTUD1. B) Co-IP of OTUD1 truncations (OTUD1-A, Ala-rich domain deletion; OTUD1-B, linker domain deletion; OTUD1-C, OTU domain deletion; and OTUD1-D, UIM domains deletion) and NRF2-Myc in HEK293T cells. C) Schematic representation of full-length and truncated NRF2. D) Co-IP of NRF2 truncations (NRF2-E, Neh2 domain deletion; NRF2-F, Neh6 domain deletion; and NRF2-G, Neh1 and 3 domains deletion) and OTUD1-Flag in HEK293T cells. E) NRF2-Myc protein levels were affected by OTUD1 truncations (OTUD1-M1, C320S inactive mutant; OTUD1-M2, ETGE deletion mutant; OTUD1-M3, C320 inactive and ETGE depletion mutant) in HEK293T cells. F) NRF2 transcriptional activity affected by OTUD1 truncations was measured by luciferase assay in HEK293T cells. G) Co-IP of OTUD1 truncations and KEAP1 in HEK293T cells. H) Co-IP of NRF2-Myc and KEAP1-Flag affected by OTUD1 truncations in HEK293T cells. For (F), the significance was determined by one-way ANOVA. $*p < 0.05$, $**p < 0.01$, $***p < 0.001$, n.s. non-significant.

motif, it is possible that OTUD1 may disrupt the interaction between KEAP1 and NRF2 by displacing NRF2 from its complex with KEAP1. Competitive IP assays showed that overexpression of OTUD1-WT and M1 obviously inhibited the interaction between NRF2 and KEAP1, whereas overexpression of M2 or M3 failed to elicit a similar effect (Fig. 5H). These data confirmed that ETGE motif of OTUD1 served as an inhibitor of KEAP1-NRF2 interaction.

In addition, our results showed that overexpression of OTUD1-WT and M1 didn't impact the protein level, subcellular localization, or total ubiquitination levels of KEAP1 in HEK293T cells (Figs. S8A–B). Subsequent analysis revealed that OTUD1 deficiency in sh-OTUD1 293T cells did not alter the total ubiquitination levels of KEAP1 (Fig. S8C), suggesting that OTUD1 does not influence the degradation of KEAP1. Moreover, our results showed that only OTUD1, and no other OTU members such as OTUD2, OTUD4, OTUD5, OTUD6B, and OTUD7B stabilized NRF2 (Fig. S9A). Taken together, these above observations indicate that OTUD1 stabilizes and activates NRF2 through its C320 catalytic residue and ETGE motif.

2.6. OTUD1 stabilizes NRF2 by inhibiting ubiquitination of NRF2

Our findings have demonstrated that OTUD1 stabilized NRF2

through its catalytic active residue C320 and ETGE motif (Fig. 5). Subsequently, we explored whether OTUD1 stabilized NRF2 by deubiquitinating it. Thus, we examined the effects of OTUD1-WT and OTUD1 mutants (M1, M2 and M3) on the overall ubiquitination of NRF2. In comparison to the robust deubiquitinating activity of OTUD1-WT on NRF2, the mutants M1 and M2 exhibited much weaker deubiquitinating activity, while the combined mutant M3 completely lacked the ability to remove ubiquitin chains from NRF2 (Fig. 6A). These results indicate that deubiquitinating activity of OTUD1 towards NRF2 necessitates both its enzymatic C320 residue and ETGE motif.

It has been reported that OTUD1 predominantly cleaved K63-linked ubiquitin from STAT3 in cardiomyocytes [29], as well as cleaving K33- and K48-chains from SMAD7 [28], and removing K6-, K11- and K29-chains from IRF3 [11]. To analyze the specific type(s) of ubiquitination of NRF2 regulated by OTUD1, we co-transfected NRF2 with each of seven K-only-ubiquitin constructs containing only the indicated lysine while the remaining six lysine residues were mutated to arginine [30]. Overexpression of OTUD1-WT significantly reduced the levels of K11-, K27- and K48-linked ubiquitination on NRF2 (Fig. 6B), indicating a coordinated impact on NRF2 stability and function. Additionally, our results also showed that C320 residue of OTUD1 was essential for cleaving polyubiquitin chains linked to K11-, K27- and K48-, while the ETGE motif specifically reducing K48-linked ubiquitination on NRF2 (Fig. 6C). Furthermore, we generated a Ub-3KR-HA plasmid (K11, K27 and K48 were mutated to R), and observed no effect of OTUD1 on the 3KR ubiquitination of NRF2 (Fig. 6D). Collectively, this data supports that OTUD1 stabilizes and activates NRF2 by removing K11-, K27- and K48- linked ubiquitin chains from NRF2.

To fully confirm the impact of OTUD1 on NRF2 stability and activity by regulating its ubiquitination state, we conducted further assessments in sh-OTUD1 293T cells. Our findings revealed that OTUD1 deficiency led to a downregulation in NRF2 transcriptional activity, a reduction in NRF2 protein level, an elevation in NRF2 ubiquitination status, and an enhanced interaction between NRF2 and KEAP1 (Figs. S10A–D).

We also tested the effect of OTUD1 mutants on H/R induced changes of apoptosis, MMP and ROS in AML12 cells. As expected, OTUD1 reduced apoptosis rate, enhanced MMP and attenuated ROS levels in AML12 under H/R conditions (Figs. S11A–E). The M1 and M2 mutants exhibited a much weaker effect, while the combined mutant M3 showed no ability to reduce apoptosis rate, enhance MMP or decrease ROS levels

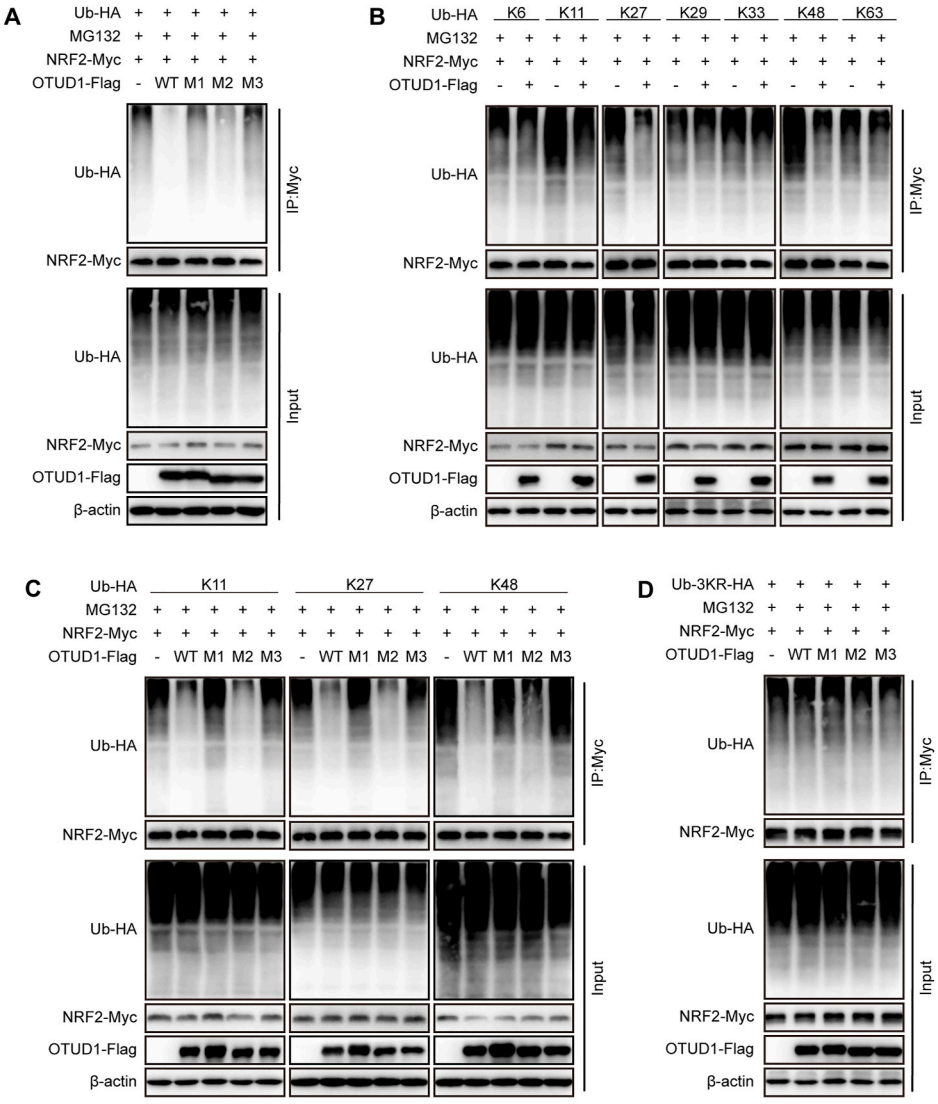

Fig. 6. OTUD1 stabilizes NRF2 by inhibiting ubiquitination of NRF2. A) HEK293T cells were transfected with the indicated plasmids, and treated with 5 μM MG132 for 12 h before collection. Denatured IP assay was performed to detect the ubiquitination of NRF2. Total ubiquitination levels of NRF2-Myc were affected by OTUD1 mutants in HEK293T cells. B) K6-, K11-, K27-, K29-, K33-, K48- and K63-linked ubiquitination levels of NRF2-Myc were affected by OTUD1-Flag in HEK293T cells. C) K11-, K27- and K48-linked ubiquitination levels of NRF2-Myc were affected by OTUD1 mutants in HEK293T cells. D) 3 KR-linked ubiquitination levels of NRF2-Myc were affected by OTUD1 mutants in HEK293T cells. $^{*}p < 0.05$, $^{**}p < 0.01$, $^{***}p < 0.001$, n.s. non-significant.

(Figs. S11A–E). These results are consistent with our previous findings and provide additional evidence for the antioxidant role of OTUD1 by stabilizing and activating NRF2.

2.7. The ETGE peptides derived from OTUD1 alleviate hepatic I/R injury

According to the aforementioned findings, the ETGE motif of OTUD1 functioned as an inhibitor of NRF2-KEAP1 interaction and facilitated the stabilization of NRF2. Subsequently, we sought to determine whether OTUD1-derived ETGE peptides (FITC-C6-AAPEPETGE) exhibited a therapeutic effect in hepatic I/R injury.

MicroScale Thermophoresis (MST) experiment revealed that the ETGE peptides bound to KEAP1 protein with an affinity constant Kd value of 11.7 μM (Fig. S12A). The flow cytometry assay demonstrated the internalization of ETGE peptides by primary hepatocytes, as evidenced by the fluorescence intensity of FITC upon incubation with the FITC-labeled peptides (Fig. S12B). To assess whether exogenous OTUD1-derived ETGE peptides can mitigate hepatocyte injury from H/R injury, primary hepatocytes were exposed to either the ETGE peptides or scramble peptides (FITC-C6-PEAPATEEG, serving as a control peptide), followed by H/R treatment. Flow cytometry results showed that the ETGE peptides attenuated H/R-induced apoptosis (Figs. S12C–D). Western blot analysis revealed elevated protein levels of Nrf2, Ho-1 and Nqo1 upon treatment with the ETGE peptides (Fig. S12E).

In order to assess the *in vivo* efficacy of ETGE peptides, mice were intravenously injected with varying doses (5, 10, and 15 mg/kg) of either ETGE peptides or scramble peptides via the tail vein and subjected to hepatic I/R treatment (Fig. 7A). The results showed that ETGE peptides, dose-dependently reduced serum ALT and AST levels, compared to scramble peptides. Notably, the highest dose of 15 mg/kg ETGE peptides

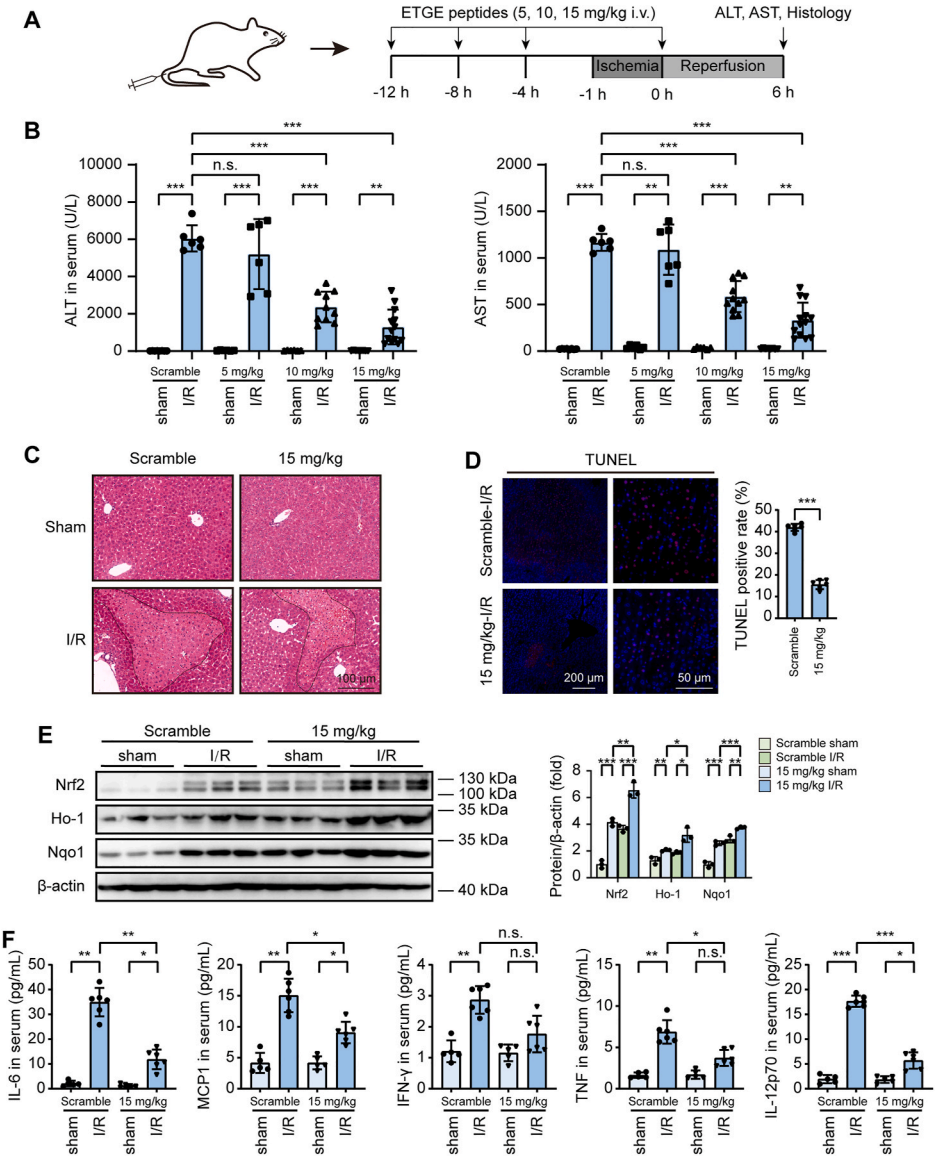

Fig. 7. The ETGE peptides derived from OTUD1 alleviate hepatic I/R injury. A) Schematic diagram of treatment of ETGE peptides to *C57BL/6J* mice. B) Serum ALT and AST levels were measured in different peptides treatments mice subjected to sham or hepatic I/R (I1R6) operation (n = 8, 6, 6, 6, 6, 10, 8, 13 for scramble + sham, scramble + I/R, 5 ml/kg + sham, 5 ml/kg + I/R, 10 ml/kg + sham, 10 ml/kg + I/R, 15 ml/kg + sham, 15 ml/kg + I/R groups respectively). C) Representative histological H&E staining images of liver sections from different peptides treatments mice subjected to sham or hepatic I/R operation (n = 6/group). D) Representative TUNEL staining images of liver sections (n = 6/group). E) The protein levels of Nrf2, Ho-1 and Nqo1 in liver samples of different peptides treatments mice subjected to sham or hepatic I/R operation (n = 3/group). F) Serum inflammatory factor levels in different peptides treatments mice subjected to sham or hepatic I/R operation (n = 6/group). For (B, E, F), the significance was determined by one-way ANOVA; for (D), the significance was determined by Student's two-tailed *t*-test. $^{*}p < 0.05$, $^{**}p < 0.01$, $^{***}p < 0.001$, n.s. non-significant.

exhibited the most potent suppressive effect, while the lowest dose of 5 mg/kg had minimal effect (Fig. 7B). Furthermore, the protective role of ETGE peptides was evident from their substantial inhibition of hepatocyte necrosis and apoptosis in liver tissues subjected to I/R injury (Fig. 7C–D and S13A-B). The antioxidant properties of ETGE peptides were also confirmed by DHE staining in I/R-challenged liver tissues (Fig. S13C). In addition, treatment with 15 mg/kg ETGE peptides led to a significant increase in NRF2 levels and its downstream cytoprotective proteins in liver tissues subjected to I/R operation (Fig. 7E). Consistently, elevated levels of serum inflammatory factors induced by hepatic I/R were attenuated by administration of either 10 or 15 mg/kg ETGE peptides (Fig. 7F and S13D). Taken together, those above results demonstrate that OTUD1-derived ETGE peptides effectively mitigate hepatic I/R injury both *in vivo* and *in vitro*.

3. Discussion

Hepatic I/R is a significant contributor to liver damage and has a substantial impact on patients' outcome following liver transplantation and resection. Currently, there are no specific clinical drugs available for hepatic I/R injury due to an incomplete understanding of the underlying mechanisms. Studies have demonstrated that proteasome inhibitors exhibit therapeutic effects in murine hepatic I/R models, suggesting DUBs, which prevent protein degradation by proteasome, may also play protective roles in hepatic I/R injury [7]. Our study revealed that the DUB member OTUD1 effectively protects against hepatic I/R injury by reducing oxidative stress, apoptosis and cytokines production. Mechanic studies showed that the regulative role of OTUD1 was primarily achieved by stabilizing and activating NRF2 via its intrinsic deubiquitinase activity and ETGE motif. Moreover, ETGE peptides derived from OTUD1 alleviated hepatic I/R injury both *in vivo* and *in vitro*. Our results unequivocally demonstrate that OTUD1 prevents liver from hepatic I/R injury.

In this study, we observed a significant upregulation of OTUD1 during the reperfusion stage in liver samples from 14 patients who underwent hepatic I/R injury during hepatectomy. OTUD1 levels, whether at pre-ischemia or reperfusion stage, exhibited a negative correlation with the peak levels of ALT or AST in individual patients on POD1. Therefore, we postulated that high OTUD1 expression might help reduce damage and improve liver function during hepatic I/R injury.

The role of OTUD1 as a tumor suppressor gene has been widely acknowledged [31,32]. In addition, it has also been shown to mitigate hepatitis induced by LPS/GalN or sepsis induced by LPS [33]. *Otud1* deletion has been found to enhance the production of inflammatory factors in response to LPS or DSS [34]. Additionally, OTUD1 has been reported to regulate secretory neutrophil polarization [35]. However, there have been no studies about the role of OTUD1 in hepatic I/R-challenged injury till now. Our study demonstrates that OTUD1 not only inhibits oxidative stress and apoptosis, but also reduces cytokine production induced by hepatic I/R operation. Keeping in line with its suppressive effect on septic inflammation caused by pathogens [33,34], our findings confirm an inhibitory role for OTUD1 in sterile inflammation caused by hepatic I/R injury.

The NRF2 transcription factor is well recognized as a potent modulator in defense against oxidative stress, a hallmark of pathology of I/R injury. Some DUBs such as DUB3 and USP29, have been reported to deubiquitinate NRF2 in non-liver diseases [22,36]. OTUD1 has been demonstrated to deubiquitinate IRF3, Smurf1 etc [11,37]. However, the interplay between the antioxidant actions of NRF2 and the regulatory role of OTUD1 in liver diseases remains poorly understood. Our study elaborates that OTUD1 serves as a specific deubiquitinase targeting and stabilizing NRF2 in hepatocytes, subsequently activating its downstream cytoprotective genes with ARE under hepatic I/R injury. In other words, NRF2 acts as a direct substrate of OTUD1 to mediate the anti-inflammatory and antioxidant effect of OTUD1 in hepatic I/R injury. Our data aligns with a previous report indicating the correlation between siOTUD1 and NRF2 reduction in PANC-1 cells but without delineating underlying mechanism [38]. Our study proposes a compelling rationale for such an occurrence.

We further demonstrated that OTUD1 possessed both deubiquitinase and KEAP1-interacting activity via its C320 residue and ETGE motif respectively. The C320 residue of OTUD1 was crucial for cleaving K11-, K27- and K48-linked ubiquitin chains from NRF2, while the ETGE motif of OTUD1 contributed to reduce K48-linked ubiquitination of NRF2 by competing with NRF2 for KEAP1-binding. K48-linked chains are the predominant linkage type in cells, while K11-linked ubiquitination is considered as an 'atypical' ubiquitin modification [39]. Their roles are to target proteins to the proteasome for degradation, providing a reasonable explanation for the positive regulation of OTUD1 upon NRF2 in our study. As for the specific significance of OTUD1 in cleaving K27-linked ubiquitination from NRF2 needs further study under hepatic I/R conditions. In addition, a recent study showed that OTUD1 regulated K63-linked ubiquitin chains from KEAP1 and NF-κB activators such as NEMO and RIP1, subsequently modulated KEAP1-mediated oxeiptosis and the NF-κB pathway [33]. In contrast to this data, OTUD1 failed to change the total ubiquitination levels of KEAP1 in our study, suggesting that specific ubiquitin-linkage cleaved by OTUD1 depend on the context. In short, OTUD1 prefers abolishing proteosome-mediated NRF2 degradation rather than modulating NRF2 function through removing K63 polyubiquitin scaffold.

Due to its robust cytoprotective role in preventing oxidative stress and inflammation, NRF2 activation is considered a promising therapeutic strategy for numerous diseases characterized by oxidative stress [40]. NRF2 binds to KEAP1, leading to recruitment of the CUL3 E3 ubiquitin ligase for NRF2 ubiquitination and degradation [13]. Therefore, NRF2 can be activated by inhibiting the interaction between NRF2 and KEAP1. In our study, we identified OTUD1 as an activator of NRF2 by disrupting the interaction between KEAP1 and NRF2 through its ETGE motif. A recent study also reported the KEAP1-binding ability of OTUD1 in HEK293T cells [33]. These findings suggest that ETEG motif derived from OTUD1 may be beneficial for activating NRF2 and contributing to hepatic I/R treatment. To this end, we synthesized ETGE peptides derived from OTUD1 and applied them to treat murine hepatic I/R injury. Our results demonstrated that OTUD1-derived ETGE peptides could remarkably alleviate hepatic I/R injury *in vivo* and *in vitro*.

In conjunction with our previous work on hepatic I/R injury, our new findings provide insight into the crucial role of OTUD1 in hepatic I/R injury by stabilizing and activating NRF2. The regulatory function of OTUD1 upon NRF2 relies on its catalytic site C320 residue and ETGE motif simultaneously. Moreover, OTUD1-derived ETGE peptides serve as an activator for NRF2 through disrupting the interaction between NRF2 and KEAP1, suggesting their potential use as a powerful drug for treating hepatic I/R injury.

4. Experimental section

4.1. Human liver samples

14 human liver samples and clinical information in this study were acquired from patients with hepatectomy at Wuhan Union Hospital from May 2021 to July 2021. Pre-hepatectomy hepatic biopsies were harvested after laparotomy before hepatic portal vein occlusion (the pre-ischemia samples in Fig. 1K–M), and post-hepatectomy hepatic biopsies were obtained after the first time of reperfusion (the reperfusion samples in Fig. 1K–N and O). The ischemic time was 15 ± 5 min, and the reperfusion time was 5 min. Informed consent forms were signed before operations. Liver samples were frozen in liquid nitrogen immediately and then transferred to -80 °C for long-term storage. Human studies were approved by Ethics Committee of Wuhan Union Hospital (UHCT-IEC-SOP-016-03-01) and followed the principles of both the Declarations of Helsinki and Istanbul. All patients were evaluated for baseline characteristics including age, gender, and diagnosis.

4.2. Animals

8–10 weeks old male *C57*BL*/6J* WT mice were purchased from Vital River (Beijing, China), and *Otud1*-knockout mice (T036968, on a *C57*BL*/6J* background) were purchased from Gem Pharmatech Company (Nanjing, China). The details of genotyping of *Otud1*-knockout mice were shown in Fig. S3. The *Nrf2*-knockout mice (S-KO-03360, Cyagen Biosciences, Suzhou, China) (on a *C57*BL*/6J* background) was a gift from Dr. Ke Hu (Wuhan union hospital, Wuhan, China). The recombinant adenovirus (Ad-Otud1) and the control adenovirus (Ad-GFP) were purchased from GeneChem (Shanghai, China). Ad-GFP (5×10^9 pfu) or Ad-Otud1 (5×10^9 pfu) were injected into *C57*BL*/6J* WT mice via the tail vein at a volume of 125 μL 36 h before hepatic I/R operation [41]. The scramble (FITC-C6-PEAPATEEG) or ETGE (FITC-C6-AAPEPETGE) peptides (Bioyears, Wuhan, China) were injected into *C57*BL*/6J* WT mice via the tail vein at a volume of 100 μL four times before reperfusion (respectively at 12, 8, 4, 0 h before reperfusion) [42]. All animal experiments were approved by the Animal Care and Use Committee of Wuhan Union Hospital (IACUC Number: 2660).

4.3. Murine hepatic I/R model

Partial (70 %) hepatic ischemia was performed as previously described [43]. In brief, sodium pentobarbital (60 mg/kg; Cat: 11715; Sigma-Aldrich) was intraperitoneal injected into mice for anesthesia, and after the complete anesthesia, laparotomy was performed along the midline of the abdomen to expose the liver. Then, the portal vein, hepatic artery and bile duct were clamped to block blood supply to the partial liver for ischemia. After 1 h of ischemia, the clamp was released for reperfusion. After 6 h of reperfusion, the mice were sacrificed for the subsequent experiments. The same operation was performed on sham mice without vasculature occlusion. Mice were subjected to I1R6 model (ischemia for 1 h followed by reperfusion for 6 h).

4.4. Cell culture

HEK293T and AML12 cells were purchased from the American Type Culture Collection (ATCC). Primary hepatocytes were isolated from the livers of mice. Cells were cultured in high-glucose DMEM medium (Cat: 11965092; Gibco) supplemented with 10 % fetal bovine serum (FBS; Cat: 16140071; Gibco) and 1 % penicillin-streptomycin (PS; Cat: 10378016; Gibco) at 37 °C in 5 % CO_2.

4.5. Liver cells H/R model

H/R model was treated as previously described [26]. AML12 cells or primary hepatocytes were cultured in high-glucose DMEM medium with 10 % FBS and 1 % PS. The medium was replaced with FBS-free and glucose-free DMEM medium (Cat: 11966025; Gibco) before hypoxia, and cells were transferred to a hypoxia condition (1 % O_2, 5 % CO_2 and 94 % N_2) by ProOX C21 (Biosherix, Lacona, NY) for 6 h. After hypoxia, the medium was replaced with 10%-FBS and high-glucose DMEM medium, and cells were transferred to a normoxia condition (95 % air and 5 % CO_2) for 1 h. AML12 cells or primary hepatocytes were subjected to H6R1 treatments (hypoxia for 6 h followed by reperfusion for 1 h).

4.6. Liver damage assessment

ALT and AST levels were measured using the DRI-CHEM 4000 Chemistry Analyzer System (Heska Loveland CO) according to the manufacturer's instructions.

4.7. Hematoxylin and eosin (H&E) staining

Liver samples were fixed in 10 % formalin, dehydrated, embedded in paraffin and sliced into 5-μm-thick continuous paraffin sections. For H&E staining, the samples were stained with hematoxylin (Cat: G1004; Servicebio) for 5 min, followed by eosin (Cat: G1001; Servicebio) for 30 s. Images were captured by a light microscope (Aperio versa8, Leica Germany). Necrotic areas were calculated by Image Pro Plus software (version 6.0, Media Cybernetics, Rockville, MD, USA).

4.8. TdT-mediated dUTP nick-end labeling (TUNEL) staining

The TUNEL assay was performed to detect cell apoptosis in liver paraffin sections according to the manufacturer's protocol (Cat: G1501; Servicebio).

4.9. Isolation of primary hepatocytes and non-parenchymal cells (NPCs)

For hepatocytes isolation, the mice were anesthetized by sodium pentobarbital. After intubation in the portal vein, the liver was perfused with Hanks buffer (Cat: H6648; Merck) for 10 min a rate of 240 mL/h, followed by low-glucose DMEM medium (Cat: 11885084; Gibco) containing 15 mM HEPES, 1 % PS and 100 CDU/mL of collagenase IV (Cat: 17018029; Gibco) for 10 min. Then, the liver was excised, minced, and strained through a mesh. Hepatocytes were precipitated by centrifuging for 2 min at 50×*g* at 4 °C. Finally, hepatocytes were cultured in DMEM with 10 % FBS and 1 % PS.

For NPCs isolation, the mice were anesthetized by sodium pentobarbital. After intubation in the portal vein, the liver was perfused with 100 CDU/mL collagenase IV for 10 min a rate of 100 mL/h. Then, the liver was excised, minced, and immersion in 100 CDU/mL collagenase IV for 20 min at 37 °C. Next, the liver was strained through a mesh. The cell suspension was centrifuged 2 min at 50×*g* at 4 °C to remove the hepatocytes recovered in the pellet. The NPCs in suspension were centrifuged, resuspended in cold Histodenz (20 % in Hanks buffer; Cat: D2158; Sigma-Aldrich), overlaid with cold Hanks and centrifuged at 1500×*g* at 4 °C for 20 min. The NPCs banding at the Histodenz-Hanks interface were collected and washed in PBS buffer.

4.10. Flow cytometry

AML12 and primary hepatocyte apoptosis was tested using FITC Annexin V Apoptosis Detection Kit I (Cat: 556547; BD Biosciences) or PE Annexin V Apoptosis Detection Kit I (Cat: 559763; BD Biosciences). Mitochondrial membrane potential was tested by Enhanced mitochondrial membrane potential assay kit with 5,5′,6,6′tetrachloro-1,1′,3,3′-tetraethylbenzimidazole-carbocyanine (JC-1; Cat: C2003S; Beyotime). ROS was tested by and 5-(and-6)-chloromethyl-2′,7′-dichlorodihydrofluorescein diacetate (H2DCFDA; Cat: D399; Invitrogen) according to the manufacturer's instructions. The data were collected using a flow cytometry (Beckman Coulter, Fullerton, CA, USA) and analyzed using FlowJo software (TreeStar, Ashland, OR, USA). Serum samples were collected from mice subjected to I/R operation. A CBA mouse inflammation kit (Cat: 552364; BD Biosciences) was used to quantitatively measure interleukin-6 (IL-6), monocyte chemoattractant protein-1 (MCP-1), interferon-γ (IFN-γ), tumor necrosis factor (TNF) and interleukin-12p70 (IL-12p70) protein levels in a single serum sample. The data were collected using a flow cytometry and analyzed using FCAP Array software (version 3.0, BD Bioscience).

4.11. Plasmid construction and lentivirus packaging

The entire human OTUD1 or murine Otud1 cDNA was cloned into the modified pHAGE-Flag-puro (pHAGE-puro, #118692, Addgene, with a 3 × Flag tag after the multiple cloning site) to express the Flag-tagged OTUD1 or Flag-tagged Otud1 recombinant protein. The entire human KEAP1 cDNA was cloned into the modified pcDNA5-HA (pcDNA5/FRT/TO V5, #19445, Addgene, with a HA tag in place of V5 tag). Various truncated forms of OTUD1 (M1, M2, M3, A, B, C, D) were amplified using overlap PCR and cloned into pHAGE-Flag-puro and pcDNA5-HA.

Various truncated forms of NRF2 (WT, E, F, G) were amplified using overlap PCR and cloned into pcDNA5-Myc. Various ubiquitin vectors were kindly provided by Xiao-Dong Zhang (Hengyang Medical School, Hengyang, China). Double-stranded oligonucleotides corresponding to the target sequences were cloned into pLKO.1 (#8453; Addgene). Overexpression or knockdown cells were obtained via lentiviral pHAGE-Flag-puro or pLKO.1 vector. In brief, the recombinant plasmids with psPAX2 (#12260; Addgene) and pMD2.G (#12259; Addgene) were co-transfected into 293T cells. Viral supernatants were harvested 48 h later and used for infecting the target cells with 8 μg/ml polybrene. The infected cells were selected with puromycin and used for gene or protein detection. All PCR primers used in this study are listed in Supplementary Table 2.

4.12. Quantitative real-time PCR

Total RNA was extracted from cells and tissues using TRIzol reagent (Cat: 15596026; Invitrogen). RNA concentrations and purity were detected using a Nano-300 (Wuhan Avist Technology, Wuhan, China), and RNA integrity was detected using agarose gel electrophoresis. cDNA was synthesized with 2 μg RNA using RevertAid First Strand cDNA Synthesis Kit (Cat: K1622; Thermo). qPCR analyses were performed using ChamQ SYBR qPCR Master Mix (Cat: Q311-02; Vazyme, Nanjing, China) to quantify mRNA expressions. All qPCR primers used in this study are listed in Supplementary Table 3.

4.13. Western blot

In this study, cells and tissues were lysed in RIPA lysis buffer (Cat: P0013B; Beyotime) at 4 °C for 15 min and centrifuged at 12,000 rpm for 15 min at 4 °C, and then the supernatants were added with loading buffer and boiled at 95 °C for 15 min. Protein concentrations were measured using a BCA protein assay kit (Cat: P0012S; Beyotime) and the absorbance was detected in 562 nm. Protein samples were separated by 10 % sodium dodecyl sulfate-polyacrylamide gel electrophoresis (SDS-PAGE) and then transferred onto polyvinylidene fluoride (PVDF) membranes (Cat: IPVH00010; Millipore). The membranes were blocked by 5 % BSA at room temperature for 30 min and incubated with primary antibodies at 4 °C overnight, followed by incubation with corresponding secondary antibodies. A ChemiScope 6000 Series (Clinx Science Instruments Co., Ltd., Shanghai, China) was used to detect protein signals. Chemiscope Image Analysis Software was used to quantify protein levels. Primary antibodies for OTUD1 (abcam, ab122481), Bcl2 (ABclonal, A0208), Bax (CST, 2772), C-caspase3 (CST, 9664), Caspase3 (CST, 9662), C-PARP (CST, 5625), PARP (CST, 9532), NRF2 (CST, 12721), HO-1 (ABclonal, A1346), NQO1 (ABclonal, A0047), KEAP1 (ABclonal, A1820), β-actin (CST, 4970), GAPDH (ABclonal, AC002), Histone H3 (CST, 4499), Flag (MBL, M185-3), Myc (MBL, M192-3) and HA (MBL, M180-3) were used for western blot analysis.

4.14. Co-immunoprecipitation (co-IP)

A co-IP assay was performed to identify the binding capacity between proteins. For the co-IP assay, HEK293T cells were co-transfected with the indicated plasmids, and PEI MAX (Cat: 24765-1; Polysciences) was used as the transfection reagent according to the manufacturer's instructions. The medium was replaced at 6 h after transfection, and cells were lysed in cold IP buffer (20 mM Tris-HCl, pH 7.4, 150 mM NaCl, 1 mM EDTA, 1 % Triton X-100 and protease inhibitor cocktail (Cat: 04693132001; Roche)) for 15 min at 4 °C at 48 h after transfection. The lysate was centrifuged at 12,000 rpm for 15 min at 4 °C. One tenth of the lysate was used as input, and the rest lysate was incubated with rProtein A/G Beads 4FF (Cat: SA032025; Smart-Lifesciences) and 1 μg of the corresponding antibody overnight at 4 °C. The beads were washed three times with cold IP buffer and the immunoprecipitated proteins were analyzed by western blot analysis.

4.15. Luciferase reporter assay

The binding elements of 44 transcription factors were cloned into the pGL3-basic vector. For the luciferase assay, HEK293T cells were co-transfected with the indicated plasmids, and PEI MAX was used as the transfection reagent. The medium was replaced at 6 h after transfection, and cells were lysed by a Dual-Luciferase Reporter Assay System kit (Cat: E1910; Promega) at room temperature for 30 min. The activity of each pathway was detected by a fluorescence detector (Promega GloMax 20/20, USA) as the manufacturer's protocol described.

4.16. Denatured immunoprecipitation assay

To detect the ubiquitination of NRF2, denatured immunoprecipitation assay was performed. HEK293T cells were transfected with the indicated plasmids, and treated with 5 μM MG132 (Cat: HY-13259; MCE) for 12 h before collection. Cells were lysed with 300 μL of SDS lysis buffer (10 % SDS in PBS) and denatured at 95 °C. Next, 600 μL of modified RIPA buffer (50 mM Tris-HCl pH 7.4, 150 mM NaCl, 1 mM EDTA, and protease inhibitor cocktail) was added to the lysates. Then, the lysates were cooled on ice for 1 h and centrifuged at 18,000 g for 30 min at 4 °C. At last, the supernatant was detected by immunoprecipitation and western blot assays.

4.17. Statistical analysis

Statistical analysis was performed by SPSS software, and the data are expressed as the mean ± standard deviation (SD). Shapiro-Wilk test was performed to assess for data normality. Student's two-tailed *t*-test was performed to compare the differences between two groups. Statistical differences among more than two groups were compared using a one-way Analysis of Variance (ANOVA), followed by Bonferroni's post hoc test (for data of homogeneity of variance) or Tamhane's T2 post hoc test (for data of heteroscedasticity of variance). Kruskal-Wallis nonparametric analysis was performed for nonnormal distribution data among multiple groups. $^{n.s.}p$ not significant, $^{*}p < 0.05$, $^{**}p < 0.01$ and $^{***}p < 0.001$. $p < 0.05$ was considered significant. Spearman correlation analysis was employed for analyzing the strength and direction of the linear relationship between two variables and represented as R^2 value (square of the Spearman correlation coefficient R).

Data availability statement

The data that support the findings of this study are available from the corresponding author upon reasonable request.

CRediT authorship contribution statement

Qi Zhang: Conceptualization, Data curation, Methodology, Supervision, Validation, Writing – original draft, Writing – review & editing, Formal analysis, Funding acquisition, Visualization. **Zihan Chen:** Data curation, Methodology. **Jinglei Li:** Data curation, Methodology. **Kunpeng Huang:** Data curation, Methodology. **Zhihao Ding:** Data curation, Methodology. **Biao Chen:** Methodology, Resources. **Tianxing Ren:** Resources, Visualization. **Peng Xu:** Resources. **Guoliang Wang:** Resources. **Hongji Zhang:** Methodology, Writing – original draft, Writing – review & editing. **Xiao-Dong Zhang:** Conceptualization, Data curation, Writing – original draft, Writing – review & editing. **Jinxiang Zhang:** Conceptualization, Funding acquisition, Supervision, Writing – original draft, Writing – review & editing. **Hui Wang:** Formal analysis, Supervision, Writing – original draft, Writing – review & editing, Conceptualization.

Declaration of competing interest

The authors declare no competing interests.

Acknowledgements

The authors thank Dr. Ying Liu and the Core Facility of Medical Research Institute at Wuhan University for flow cytometry and histological analysis. The authors thank Dr. Shoujun Huang (Anhui Agricultural University, Hefei, China) for the OTU family members vectors. The authors thank Dr. Ke Hu (Wuhan union hospital, Wuhan, China) for the Nrf2-knock mice. The authors thank student Bowen Zhang for some animal experiments. This study was supported by grants from the National Natural Science Foundation of China (No. 82370647, No. 82100673, No. 82170642, No. 82100662, No. 81801923, No. 81700558, No. 81570570, No. 81670575 and No. 81070355), Program of HUST Academic Frontier Youth Team (2018QYTD02), and Pre-Research Fund for Free Innovation of Union Hospital, Huazhong University of Science and Technology (No. 02.03.2017-312, No. 02.03.2017-59, and No. 02.03.2018-126).

Appendix A. Supplementary data

Supplementary data to this article can be found online at https://doi.org/10.1016/j.redox.2024.103287.

References

[1] H. Han, R. Desert, S. Das, Z. Song, D. Athavale, X. Ge, N. Nieto, Danger signals in liver injury and restoration of homeostasis, J. Hepatol. 73 (4) (2020) 933–951.
[2] V.G. Agopian, M.P. Harlander-Locke, D. Markovic, W. Dumronggittigule, V. Xia, F. M. Kaldas, A. Zarrinpar, H. Yersiz, D.G. Farmer, J.R. Hiatt, R.W. Busuttil, Evaluation of early allograft function using the liver graft assessment following transplantation risk score model, JAMA Surg 153 (5) (2018) 436–444.
[3] A. Hofer, D. Jonigk, B. Hartleben, M. Verboom, M. Hallensleben, S.G. Hubscher, M. P. Manns, E. Jaeckel, R. Taubert, DSA are associated with more graft injury, more fibrosis, and upregulation of rejection-associated transcripts in subclinical rejection, Transplantation 104 (3) (2020) 551–561.
[4] Y. Liu, T. Lu, C. Zhang, J. Xu, Z. Xue, R.W. Busuttil, N. Xu, Q. Xia, J.W. Kupiec-Weglinski, H. Ji, Activation of YAP attenuates hepatic damage and fibrosis in liver ischemia-reperfusion injury, J. Hepatol. 71 (4) (2019) 719–730.
[5] M. Ni, J. Zhang, R. Sosa, H. Zhang, H. Wang, D. Jin, K. Crowley, B. Naini, F.E. Reed, R.W. Busuttil, J.W. Kupiec-Weglinski, X. Wang, Y. Zhai, T-cell immunoglobulin and mucin domain-containing protein-4 is critical for kupffer cell homeostatic function in the activation and resolution of liver ischemia reperfusion injury, Hepatology 74 (4) (2021) 2118–2132.
[6] C. Pohl, I. Dikic, Cellular quality control by the ubiquitin-proteasome system and autophagy, Science 366 (6467) (2019) 818–822.
[7] N. Alva, A. Panisello-Rosello, M. Flores, J. Rosello-Catafau, T. Carbonell, Ubiquitin-proteasome system and oxidative stress in liver transplantation, World J. Gastroenterol. 24 (31) (2018) 3521–3530.
[8] S.M. Lange, L.A. Armstrong, Y. Kulathu, Deubiquitinases: from mechanisms to their inhibition by small molecules, Mol. Cell 82 (1) (2022) 15–29.
[9] Z. Chen, F. Hu, Y. Zhang, L. Zhang, T. Wang, C. Kong, H. Hu, J. Guo, Q. Chen, B. Yu, Y. Liu, J. Zou, J. Zhou, T. Qiu, Ubiquitin-specific protease 29 attenuates hepatic ischemia-reperfusion injury by mediating TGF-beta-activated kinase 1 deubiquitination, Front. Immunol. 14 (2023) 1167667.
[10] H. Liu, J. Fan, W. Zhang, Q. Chen, Y. Zhang, Z. Wu, OTUD4 alleviates hepatic ischemia-reperfusion injury by suppressing the K63-linked ubiquitination of TRAF6, Biochem. Biophys. Res. Commun. 523 (4) (2020) 924–930.
[11] Z. Zhang, D. Wang, P. Wang, Y. Zhao, F. You, OTUD1 negatively regulates type I IFN induction by disrupting noncanonical ubiquitination of IRF3, J. Immunol. 204 (7) (2020) 1904–1918.
[12] D. Lu, J. Song, Y. Sun, F. Qi, L. Liu, Y. Jin, M.A. McNutt, Y. Yin, Mutations of deubiquitinase OTUD1 are associated with autoimmune disorders, J. Autoimmun. 94 (2018) 156–165.
[13] A. Cuadrado, A.I. Rojo, G. Wells, J.D. Hayes, S.P. Cousin, W.L. Rumsey, O. C. Attucks, S. Franklin, A.L. Levonen, T.W. Kensler, A.T. Dinkova-Kostova, Therapeutic targeting of the NRF2 and KEAP1 partnership in chronic diseases, Nat. Rev. Drug Discov. 18 (4) (2019) 295–317.
[14] Z. Yi, M. Deng, M.J. Scott, G. Fu, P.A. Loughran, Z. Lei, S. Li, P. Sun, C. Yang, W. Li, H. Xu, F. Huang, T.R. Billiar, Immune-responsive gene 1/itaconate activates nuclear factor erythroid 2-related factor 2 in hepatocytes to protect against liver ischemia-reperfusion injury, Hepatology 72 (4) (2020) 1394–1411.
[15] W. Liang, J. Greven, K. Qin, A. Fragoulis, K. Horst, F. Blasius, C. Wruck, T. Pufe, P. Kobbe, F. Hildebrand, P. Lichte, Sulforaphane exerts beneficial immunomodulatory effects on liver tissue via a Nrf2 pathway-related mechanism in a murine model of hemorrhagic shock and resuscitation, Front. Immunol. 13 (2022) 822895.
[16] B. Ke, X.D. Shen, Y. Zhang, H. Ji, F. Gao, S. Yue, N. Kamo, Y. Zhai, M. Yamamoto, R.W. Busuttil, J.W. Kupiec-Weglinski, KEAP1-NRF2 complex in ischemia-induced hepatocellular damage of mouse liver transplants, J. Hepatol. 59 (6) (2013) 1200–1207.
[17] P. Abrescia, L. Treppiccione, M. Rossi, P. Bergamo, Modulatory role of dietary polyunsaturated fatty acids in Nrf2-mediated redox homeostasis, Prog. Lipid Res. 80 (2020) 101066.
[18] J.D. Hayes, A.T. Dinkova-Kostova, The Nrf2 regulatory network provides an interface between redox and intermediary metabolism, Trends Biochem. Sci. 39 (4) (2014) 199–218.
[19] M. Yamamoto, T.W. Kensler, H. Motohashi, The KEAP1-NRF2 system: a thiol-based sensor-effector apparatus for maintaining redox homeostasis, Physiol. Rev. 98 (3) (2018) 1169–1203.
[20] M. Rojo de la Vega, E. Chapman, D.D. Zhang, NRF2 and the hallmarks of cancer, Cancer Cell 34 (1) (2018) 21–43.
[21] A. Cuadrado, G. Manda, A. Hassan, M.J. Alcaraz, C. Barbas, A. Daiber, P. Ghezzi, R. Leon, M.G. Lopez, B. Oliva, M. Pajares, A.I. Rojo, N. Robledinos-Anton, A. M. Valverde, E. Guney, H. Schmidt, Transcription factor NRF2 as a therapeutic target for chronic diseases: a systems medicine approach, Pharmacol. Rev. 70 (2) (2018) 348–383.
[22] Q. Zhang, Z.Y. Zhang, H. Du, S.Z. Li, R. Tu, Y.F. Jia, Z. Zheng, X.M. Song, R.L. Du, X.D. Zhang, DUB3 deubiquitinates and stabilizes NRF2 in chemotherapy resistance of colorectal cancer, Cell Death Differ. 26 (11) (2019) 2300–2313.
[23] C. Meng, J. Zhan, D. Chen, G. Shao, H. Zhang, W. Gu, J. Luo, The deubiquitinase USP11 regulates cell proliferation and ferroptotic cell death via stabilization of NRF2 USP11 deubiquitinates and stabilizes NRF2, Oncogene 40 (9) (2021) 1706–1720.
[24] H. Zhang, J. Goswami, P. Varley, D.J. van der Windt, J. Ren, P. Loughran, H. Yazdani, M.D. Neal, R.L. Simmons, J. Zhang, A. Tsung, H. Huang, Hepatic surgical stress promotes systemic immunothrombosis that results in distant organ injury, Front. Immunol. 11 (2020) 987.
[25] L. Zhang, J. Liu, L. Qian, Q. Feng, X. Wang, Y. Yuan, Y. Zuo, Q. Cheng, Y. Miao, T. Guo, X. Zheng, H. Zheng, Induction of OTUD1 by RNA viruses potently inhibits innate immune responses by promoting degradation of the MAVS/TRAF3/TRAF6 signalosome, PLoS Pathog. 14 (5) (2018) e1007067.
[26] W.M. Pan, H. Wang, X.F. Zhang, P. Xu, G.L. Wang, Y.J. Li, K.P. Huang, Y.W. Zhang, H. Zhao, R.L. Du, H. Huang, X.D. Zhang, J.X. Zhang, miR-210 participates in hepatic ischemia reperfusion injury by forming a negative feedback loop with SMAD4, Hepatology 72 (6) (2020) 2134–2148.
[27] C.F. Bennett, P. Latorre-Muro, P. Puigserver, Mechanisms of mitochondrial respiratory adaptation, Nat. Rev. Mol. Cell Biol. 23 (12) (2022) 817–835.
[28] Z. Zhang, Y. Fan, F. Xie, H. Zhou, K. Jin, L. Shao, W. Shi, P. Fang, B. Yang, H. van Dam, P. Ten Dijke, X. Zheng, X. Yan, J. Jia, M. Zheng, J. Jin, C. Ding, S. Ye, F. Zhou, L. Zhang, Breast cancer metastasis suppressor OTUD1 deubiquitinates SMAD7, Nat. Commun. 8 (1) (2017) 2116.
[29] M. Wang, X. Han, T. Yu, M. Wang, W. Luo, C. Zou, X. Li, G. Li, G. Wu, Y. Wang, G. Liang, OTUD1 promotes pathological cardiac remodeling and heart failure by targeting STAT3 in cardiomyocytes, Theranostics 13 (7) (2023) 2263–2280.
[30] R. Tu, W. Kang, X. Yang, Q. Zhang, X. Xie, W. Liu, J. Zhang, X.D. Zhang, H. Wang, R.L. Du, USP49 participates in the DNA damage response by forming a positive feedback loop with p53, Cell Death Dis. 9 (5) (2018) 553.
[31] F. Yao, Z. Zhou, J. Kim, Q. Hang, Z. Xiao, B.N. Ton, L. Chang, N. Liu, L. Zeng, W. Wang, Y. Wang, P. Zhang, X. Hu, X. Su, H. Liang, Y. Sun, L. Ma, SKP2- and OTUD1-regulated non-proteolytic ubiquitination of YAP promotes YAP nuclear localization and activity, Nat. Commun. 9 (1) (2018) 2269.
[32] Q. Luo, X. Wu, P. Zhao, Y. Nan, W. Chang, X. Zhu, D. Su, Z. Liu, OTUD1 activates caspase-independent and caspase-dependent apoptosis by promoting AIF nuclear translocation and MCL1 degradation, Adv. Sci. 8 (8) (2021) 2002874.
[33] D. Oikawa, M. Gi, H. Kosako, K. Shimizu, H. Takahashi, M. Shiota, S. Hosomi, K. Komakura, H. Wanibuchi, D. Tsuruta, T. Sawasaki, F. Tokunaga, OTUD1 deubiquitinase regulates NF-kappaB- and KEAP1-mediated inflammatory responses and reactive oxygen species-associated cell death pathways, Cell Death Dis. 13 (8) (2022) 694.
[34] B. Wu, L. Qiang, Y. Zhang, Y. Fu, M. Zhao, Z. Lei, Z. Lu, Y.G. Wei, H. Dai, Y. Ge, M. Liu, X. Zhou, Z. Peng, H. Li, C.P. Cui, J. Wang, H. Zheng, C.H. Liu, L. Zhang, The deubiquitinase OTUD1 inhibits colonic inflammation by suppressing RIPK1-mediated NF-kappaB signaling, Cell. Mol. Immunol. 19 (2) (2022) 276–289.
[35] J. Song, Y. Zhang, Y. Bai, X. Sun, Y. Lu, Y. Guo, Y. He, M. Gao, X. Chi, B.C. Heng, X. Zhang, W. Li, M. Xu, Y. Wei, F. You, X. Zhang, D. Lu, X. Deng, The deubiquitinase OTUD1 suppresses secretory neutrophil polarization and ameliorates immunopathology of periodontitis, Adv. Sci. 10 (30) (2023) e2303207.
[36] W. Liu, P. Tang, J. Wang, W. Ye, X. Ge, Y. Rong, C. Ji, Z. Wang, J. Bai, J. Fan, G. Yin, W. Cai, Extracellular vesicles derived from melatonin-preconditioned mesenchymal stem cells containing USP29 repair traumatic spinal cord injury by stabilizing NRF2, J. Pineal Res. 71 (4) (2021) e12769.
[37] S. Wang, P. Hou, W. Pan, W. He, D.C. He, H. Wang, H. He, DDIT3 targets innate immunity via the DDIT3-OTUD1-MAVS pathway to promote bovine viral diarrhea virus replication, J. Virol. 95 (6) (2021) e02351, 02320.
[38] M. Grattarola, M.A. Cucci, A. Roetto, C. Dianzani, G. Barrera, S. Pizzimenti, Post-translational down-regulation of Nrf2 and YAP proteins, by targeting deubiquitinases, reduces growth and chemoresistance in pancreatic cancer cells, Free Radic. Biol. Med. 174 (2021) 202–210.
[39] Y.T. Kwon, A. Ciechanover, The ubiquitin code in the ubiquitin-proteasome system and autophagy, Trends Biochem. Sci. 42 (11) (2017) 873–886.
[40] A. Cuadrado, Brain-protective mechanisms of transcription factor NRF2: toward a common strategy for neurodegenerative diseases, Annu. Rev. Pharmacol. Toxicol. 62 (2022) 255–277.
[41] J. Wang, H.W. Koh, L. Zhou, U.J. Bae, H.S. Lee, I.H. Bang, S.O. Ka, S.H. Oh, E. J. Bae, B.H. Park, Sirtuin 2 aggravates postischemic liver injury by deacetylating

mitogen-activated protein kinase phosphatase-1, Hepatology 65 (1) (2017) 225–236.

[42] S.Z. Li, Q.P. Shu, Y. Song, H.H. Zhang, Y. Liu, B.X. Jin, T.Z. Liuyu, C. Li, X. C. Huang, R.L. Du, W. Song, B. Zhong, X.D. Zhang, Phosphorylation of MAVS/VISA by Nemo-like kinase (NLK) for degradation regulates the antiviral innate immune response, Nat. Commun. 10 (1) (2019) 3233.

[43] W. Pan, L. Wang, X.F. Zhang, H. Zhang, J. Zhang, G. Wang, P. Xu, Y. Zhang, P. Hu, X.D. Zhang, R.L. Du, H. Wang, Hypoxia-induced microRNA-191 contributes to hepatic ischemia/reperfusion injury through the ZONAB/Cyclin D1 axis, Cell Death Differ. 26 (2) (2019) 291–305.